Astron. Astrophys. 352, 567–573 (1999)

ASTRONOMY AND ASTROPHYSICS

The density of methane brown dwarfs: observational and theoretical constraints

F. D'Antona[1], **E. Oliva**[2], **and A. Zeppieri**[1]

[1] Osservatorio Astronomico di Roma, Monte Porzio Catone, 00040 Roma, Italy
[2] Osservatorio Astrofisico di Arcetri, Largo E. Fermi 5, 50125 Firenze, Italy

Received 18 June 1999 / Accepted 1 October 1999

Abstract. Methane brown dwarfs (CH_4BDs), i.e. objects similar to the low mass star Gliese 229B, are characterized by very unusual colours: J–K$\lesssim$0 and I–J$\gtrsim$5. An analysis of the ESO public images, which cover an area of 37 sq. arcmin in the three filters, yields one clear CH_4BD candidate with J=20.2 and two fainter sources with J$\simeq$23. The resulting observed density of methane dwarfs ranges from $\approx$100 to $\approx$500 objects per sq. degree with J$<$23.1, quite high but compatible, within the errors, with what we derive from simulations of the stellar population of brown dwarfs in the disk of the Galaxy adopting reasonable (although still speculative) hypotheses on the evolution of BD colours with cooling. The predictions presented here can be useful in constraining the results from future searches of these objects in the infrared. Deep imaging of several sq. degrees of sky down to J$\simeq$22, K$\simeq$22 and I$\gtrsim$27 are necessary to significantly improve the observational database.

Key words: stars: low-mass, brown dwarfs – stars: luminosity function, mass function – infrared: stars

1. Introduction

Until recently, only three very low luminosity objects were known with spectral type later than M9.5, but the two near IR ground based surveys DENIS and 2MASS opened a new window in the study of the end of the main sequence and its continuation into the realm of Brown Dwarfs (BDs). In fact, DENIS added three objects (Delfosse et al. 1999, Tinney et al. 1998), and 2MASS (Kirkpatrick et al. 1998) increased this sample till now by about 20 objects spectroscopically confirmed by the Low Resolution Infrared Spectrometer at Keck. These findings are defining a new spectral class, the "L dwarfs" spanning $T_{\rm eff}\sim$2200–1500 K, their exact temperatures depending on the treatment of dust in model atmospheres.

It was recently recognized that the near IR colours of the late M dwarfs ($T_{\rm eff}\lesssim$2600 K) could not be reproduced by model atmospheres, unless they included consideration of grains. Although the spectral features are very complex, the first generation of model atmospheres including grain condensations (Tsuji et al. 1996, Allard 1998) are able to interpret the main emerging spectral characteristics, and include predictions also for the L–dwarf spectra. Dust grains forming in the upper layers of very cool dwarfs have a large opacity, and produce a redistribution of the IR flux (greenhouse effect), explaining the very red J–K colours of the latest M and of the L-dwarfs. The L–dwarfs clearly define the low end of the MS, which, depending on the opacity, and thus on the dust inclusion in the models, may be shifted to even as low as $\sim$1800 K (Burrows & Sharp 1999). However, due to the steepness of the mass luminosity relation around the hydrogen burning minimum mass (D'Antona & Mazzitelli 1985), the range of $T_{\rm eff}$'s of L-dwarfs should be mostly populated by cooling brown dwarfs. An indication confirming this interpretation is the presence of Lithium in about half of the 2MASS objects, indicating that they are unable to burn their initial lithium, and thus that their mass is below $\sim$0.06 $M_\odot$ (see however Allard 1998 for a different interpretation).

When L-dwarfs evolve further, they will eventually reach $T_{\rm eff}<$1500 K. Just as for normal white dwarfs, the evolutionary time is dictated by the release of the thermal energy of the ions, so that it increases when decreasing the luminosity. Only one object was until recently identified as the result of such cooling: the companion to the low mass star Gliese 229, having a spectrum showing the CH_4 bands, predicted by theory. This object, the "Rosetta stone" of cool BDs, at $T_{\rm eff}\sim$900 K and luminosity well below $10^{-5}L_\odot$ (Leggett et al. 1999), shows in fact a peculiar spectrum characterized by metal depletions, and dominated by H_2O, CH_4 and alkali metals. The flux redistribution at very low $T_{\rm eff}$ produces a spectrum much bluer in J–K, while keeping a very red I–K colour (e.g. Burrows et al. 1997). Therefore, while the typical colour of L–dwarfs are J–K$>$1.3 (e.g. Leggett et al. 1998), the cooler BDs should have J–K$\simeq$0, as confirmed by the colour of Gliese 229B (Nakajima et al. 1995, Leggett et al. 1999).

Although this outline of low mass and brown dwarf evolution is qualitatively sound, we are quite far from a complete theoretical understanding of the problem. At the upper mass end ($M\gtrsim 0.4M_\odot$) the inclusion of molecular opacities in the model atmospheres, and the use of boundary conditions from non-gray model atmospheres for the interior models has improved considerably the match between the stellar models and the observed colour of stars (see Baraffe et al. 1998, hereafter B98). We have

Send offprint requests to: F. D'Antona
(dantona@coma.mporzio.astro.it)

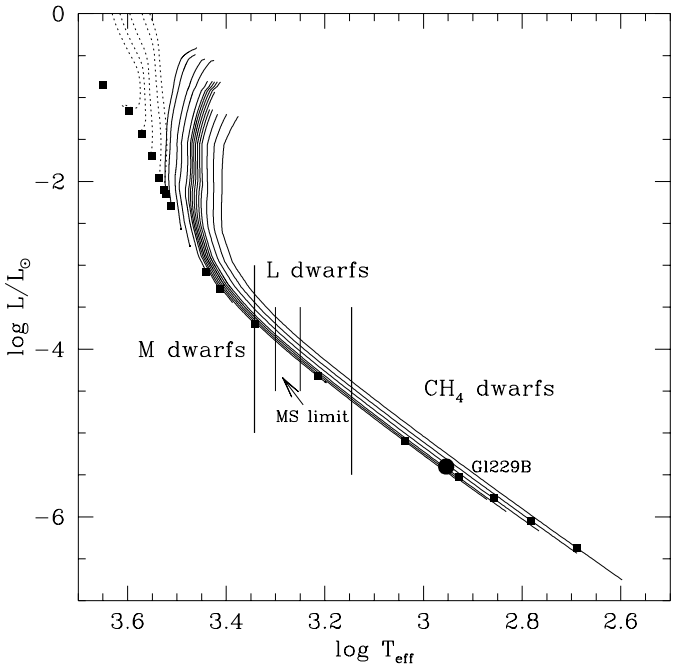

Fig. 1. HR diagram with the evolutionary tracks of low mass stars. The dashed lines are from D'Antona & Mazzitelli (1997) and cover the 0.6 to 0.2 $M_{\odot}$ range, while the tracks for lower mass stars (0.237 to 0.03 $M_{\odot}$) are from Burrows et al. (1998). The square symbols mark the positions at 10^{10} years. The approximate boundaries of the M, L and methane dwarfs are shown. The Main Sequence limit is between 2000 and 1800 K depending on the opacities adopted, so it falls in the middle of the L spectral type.

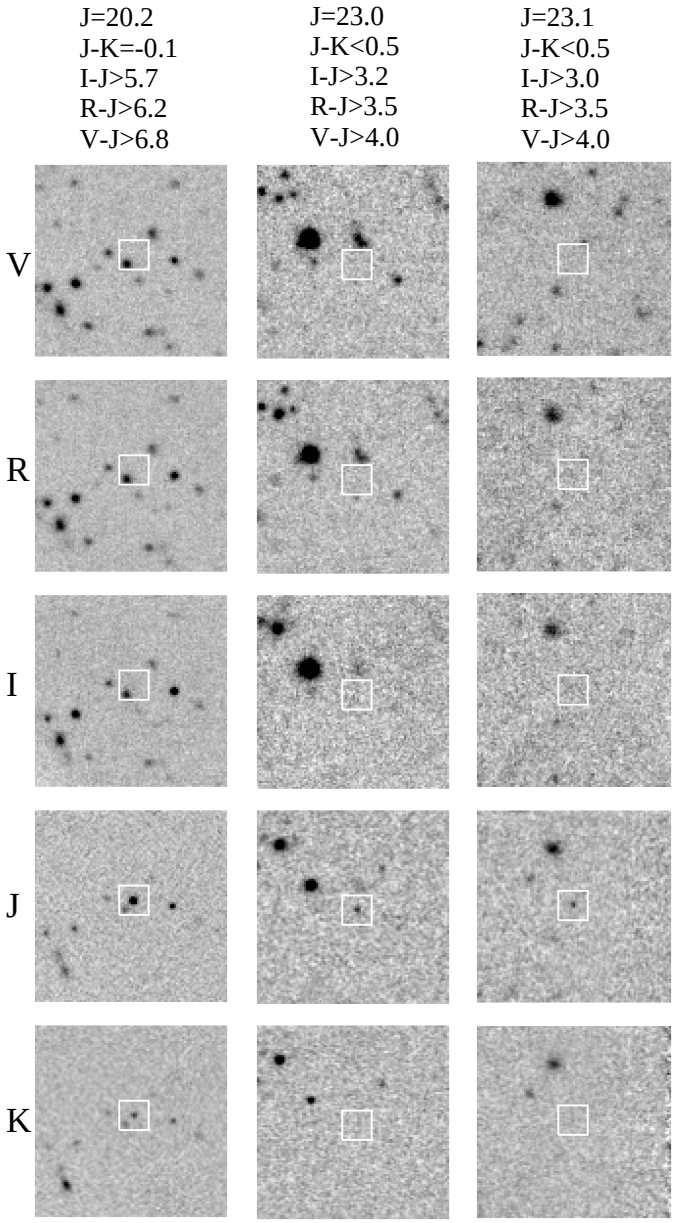

Fig. 2. Selected regions of the ESO deep fields showing the CH_4BDs candidates. Each sub-frame is 28″x28″ with N to the left and E to the bottom, the position of the candidate is marked by a white rectangle. The magnitudes and colours are $\pm$0.15 while the upper/lower limits are at the 3σ level.

remarked that the optical colours at $T_{\rm eff}$<2500 K require grain inclusion in the models. This is a difficult task, although insight is expected based on the "dusty" modeling by Allard (1998) and on the grain clouds approach by Burrows et al. (1998). Nevertheless, the unknowns in the modeling of grains (e.g. the particle size distribution, the spatial distribution of clouds, their composition, or the assumption of chemical equilibrium without rain–out) shift very far away in time a self–consistent approach. In addition, the detailed colour transition from L dwarfs to CH_4BDs can not be yet described quantitatively.

Fig. 1 shows the evolutionary tracks of dwarfs and BDs, and a very schematic separation between M, L and methane dwarfs, in terms of $T_{\rm eff}$, which we choose according to Reid et al. (1998). These limits must be taken with the caution due to the uncertainties described above.

2. Observational constraints on the density of faint CH_4BDs

In spite of all the difficulties in the models, the very blue J–K colour, together with a very red I–K, should be a signature of the very low $T_{\rm eff}$, older BDs which we will call CH_4BDs. This simple recognition has prompted us to search for faint objects characterized by small J–K but very large I–K or R–J, indicative of low $T_{\rm eff}$. A very useful data set comes from the ESO public survey data which are targeted at regions far from the galactic plane and include the NTT SUSI deep field (l=284°, b=+53°, Arnouts et al. 1999, Moorwood et al. 1998), the EIS HDF–S field (l=328°, b=−49°, da Costa et al. 1999) and the AXAF deep field (l=224°, b=−54°, Rengelink et al. 1999). The overlap between infrared (K, J) and optical (I, R, V) images cover a total area of 37 sq. arcmin and is complete to K=22.6, J=24.4 and I=26.3 mag. These limits are somewhat unbalanced for our purposes, i.e. too shallow in K and I for the depth reached in J. The colour selection we use to extract methane dwarf candidates effectively translates into a cut at J=23.1 and much above the limit of completeness of the J images.

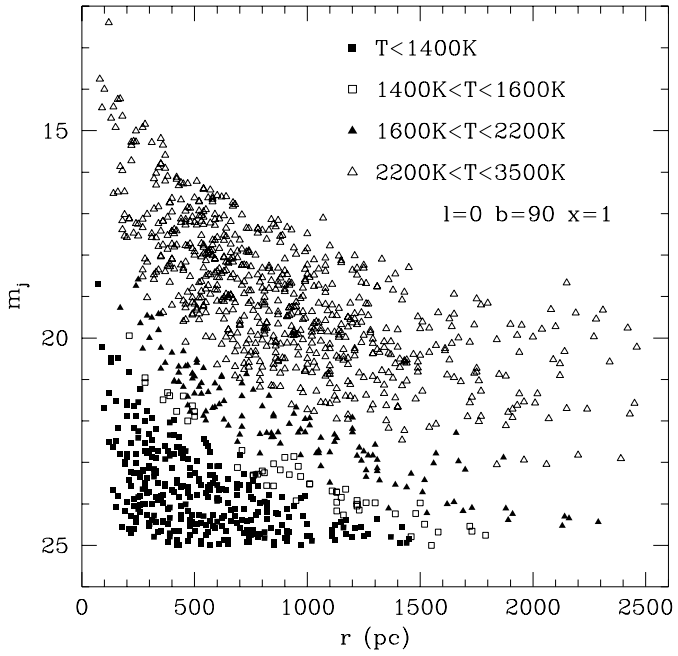

Fig. 3. Example of the predicted distribution of apparent stellar J magnitudes versus the distance, for simulated observations covering 1 square degree.

The methane dwarf candidates were selected as those point–like objects with J–K<0.5 and I–J>3, i.e. colours which are incompatible with any known stellar source other than GL229B. This yielded three objects whose finding charts and magnitudes are shown in Fig. 2. Considered the statistical errors, the corresponding density ranges between ≈100 and ≈500 objects per sq. degree with magnitudes J<23.1.

It should be noted that the colours of the selected objects are also compatible with quasars or QSOs at $z \sim 9$, i.e. at redshifts where the Lyα falls into the J band and the Lyman–break is moved beyond the I photometric band. In such a case an observed magnitude J=23 would translate into an absolute blue magnitude $\mathrm{M_B} \simeq -25$ and typical of low–medium luminosity QSOs. However, we consider this possibility unlikely because current estimates of the density of quasars at various redshifts indicate a rapid drop beyond z=3 with basically no object at $z > 6$ (e.g. Shaver et al. 1996). Encouragingly, the CH_4BD nature of the brightest object was recently confirmed by spectroscopic IR observations at the VLT (Cuby et al. 1999).

3. Modelling of number counts and predicted colours

As outlined in the introduction, it is not yet possible to model self–consistently the whole BD evolution. We decided therefore to adopt an admittedly rather simple–minded approach to the colour derivation, in order get a first estimate of the expected number counts of CH_4BDs. On the other hand, we took care to model carefully the galactic disk, so that the global model can be easily improved when more precise evolutionary tracks will be available.

Table 1. Adopted colours and bolometric corrections

$\log T_{\rm eff}$	$BC_J^{(1)}$	$(\mathrm{J–K})^{(2)}_{mod}$	$(\mathrm{J–K})^{(3)}_{emp}$
2.768	2.23[a]	–1.44[a]	–1.44
3.000	2.20[a]	–0.10[a]	–0.10
3.301	2.19	0.87	1.37
3.362	2.16	0.92	1.21
3.423	2.07	0.93	1.06
3.447	2.00	0.92	0.97
3.498	1.88	0.87	0.91
3.529	1.81	0.84	0.84
3.554	1.75	0.81	0.81
3.592	1.66	0.79	0.79
3.631	1.54	0.71	0.71
3.674	1.39	0.57	0.57
3.713	1.26	0.43	0.43

(1) Bolometric correction in J, from B98, except for those in note a
(2) Colours predicted by models, from B98 except for those in note a
(3) Empirical colours adopted here, see Sect. 3.2
[a] Values from Burrows et al. (1997)

3.1. The theoretical models

As a first input, we need the time evolution of $\log L/L_\odot$ and $T_{\rm eff}$ for stellar masses which trace the low end of the main sequence and the brown dwarf evolution. We will use as a basis the models by Burrows et al. (1997 and private communication) employing non-gray model atmospheres up to 1300 K, and similarly low-resolution, non-gray models with grains up to 2400 K. Above this temperature, gray models with Rosseland opacities from Saumon are adopted. These tracks are computed for masses from $0.237 M_\odot$ to $0.03 M_\odot$, and are evolved up to an age of 20 Gyr, which is reached at quite low $T_{\rm eff}$ for the smaller masses, so they constitute a very complete set to deal with all the very low mass and brown dwarf regimes, from the M spectral type, through the L dwarfs, to the postulated CH_4BDs phase. Above this mass, for the purpose of having predictions available also for somewhat hotter stars, we adopt the tracks by D'Antona & Mazzitelli (1997) from 0.25 to $0.8 M_\odot$. Although the latter are computed with somewhat different inputs (e.g the deuterium initial abundance is half of the abundance assumed by Burrows et al., the treatment of over–adiabatic convection is different) the merging of the two sets is very reasonable, also because mainly the main sequence or cooling part of the sequences are important to determine the stellar counts. The gray-atmosphere low-mass models by D'Antona & Mazzitelli (1997) predict luminosities larger by $\sim 15\%$ (generally < 0.1 mag) than the non gray models e.g. by Chabrier & Baraffe (1997, hereafter CB97) and have $T_{\rm eff} \sim 2\%$ larger. The Burrows et al. models above 2400 K compare well with those of CB97 in luminosity, and they differ by 2% in $T_{\rm eff}$.

3.2. Colours and bolometric corrections

The magnitudes in I, J and K are not directly available in the track sets, so we decided to adopt the admittedly crude procedure of

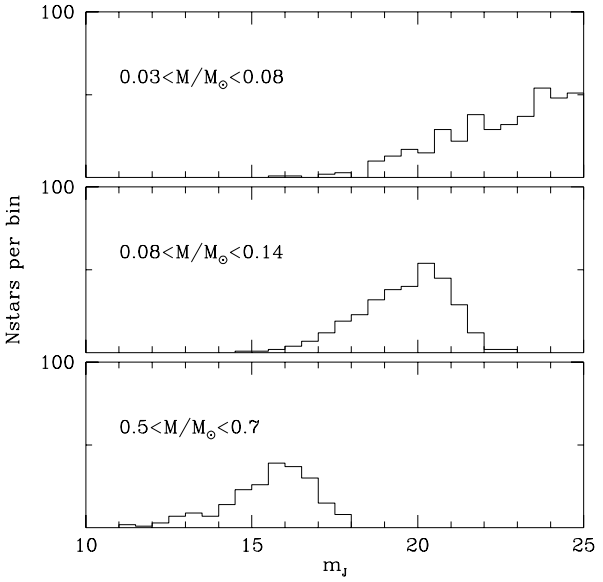

Fig. 4. Stellar counts (in bins of 0.5mag, per square degree) as function of the apparent J magnitude for three selected mass ranges.

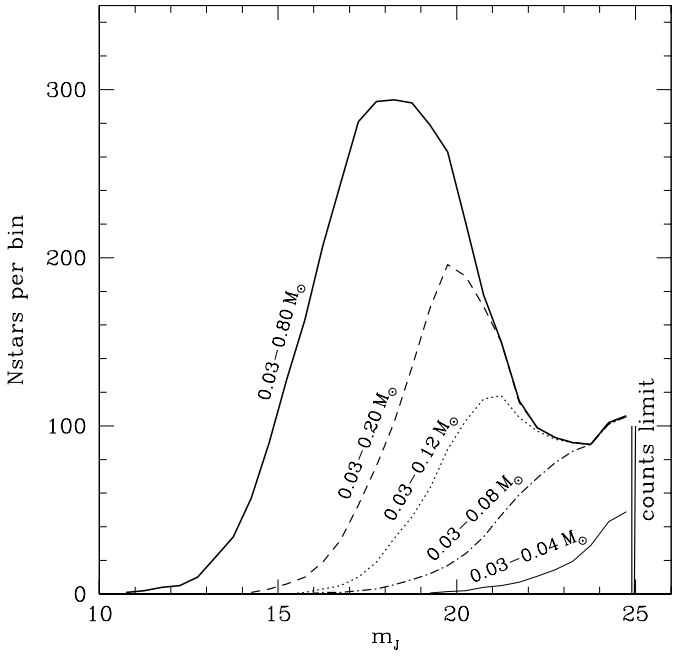

Fig. 5. Stellar counts in bins of half magnitude and per square degree as a function of the apparent magnitude J, in the case l=0, b=90, x=0. The cumulative counts from 0.03 to 0.8$M_\odot$ are shown in the thick line. Partial counts due to separate mass ranges are also given to show at which magnitudes each mass range contributes mostly to the counts. The continuous line at the lower right represents the counts from 0.03 to 0.04$M_\odot$, the dash-dotted one from 0.03 to 0.08$M_\odot$, the dotted line from 0.03 to 0.12$M_\odot$ and the dashed from 0.03 to 0.2$M_\odot$ The BD mass range is largely represented only for J>20. The counts are limited to J=25, but BDs would be present also above this magnitude.

estimating the I and J band bolometric corrections (BC) from the B98 models, which are consistent with the CB97 models. The B98 values have been used for $T_{\rm eff} > 2000$ K. We extrapolate these BCs to $T_{\rm eff}$=600 K using the models of Burrows et al. (1997). The J band counts should be little affected by uncertainties in the bolometric corrections. In fact, BC_J is 2.19mag at 2000 K, and very similar (2.23mag) at $T_{\rm eff}$=600 K (see Table 1). In other words, 25–30% of the flux for these objects emerges in the J band, regardless of their temperature (e.g. Burrows et al. 1998).

The colours J–K are taken from Burrows et al. (1998) for $T_{\rm eff} \leq$1000 K. Above 3300 K we adopt the colours of B98. In the intermediate range, these models fail reproduce the observations of cooler dwarfs (Leggett et al. 1998, B98) and computations including grains should be used (e.g. Allard 1998, Jones & Tsuji 1998) to get the very red J–K colours down to GD165B. However, dusty models are still very incomplete and we therefore employed a semiempirical approximation, imposing the models to pass through the colour of GD165B and then to evolve to the blue. Table 1 shows the adopted relation between $T_{\rm eff}$ and J–K. The reader should be well aware that this approach represents an educated guess on the CH_4BDs colour evolution. Nevertheless the semiempirical approach mainly influences the *relative* number counts of the J versus K band, but not the $T_{\rm eff}$ selection, which however is itself is uncertain in the absence of better modeling.

3.3. The integrated number counts

The number of stars within a given range of temperature ($T_{\rm eff} \pm \Delta T$) and apparent magnitude (J$\pm\Delta$J) expected from observations directed at a given direction l, b (galactic coordinates) and covering a relatively small solid angle Ω is given by

$$\Sigma(T_{\rm eff}, {\rm J}) = \int_0^\infty \Phi[T_{\rm eff}, ({\rm J} - 5\log R_{10})]\ \rho(R)\ \Omega\ R^2 dR \qquad (1)$$

where R is the distance from the sun along the l, b line of sight, R_{10}=(R/10 pc) and ρ is the total stellar density whose radial dependence can be approximated by (Bahcall & Soneira 1978)

$$\begin{aligned} \rho(R) &= \rho_o\ \exp(-z/H - (r - r_o)/h) \\ z &= R\ \sin b \\ r &= \sqrt{(R\cos b)^2 - 2Rr_o\cos b\cos l + r_o^2} \end{aligned}$$

The coordinate z is measured perpendicular to the galactic plane, r is the radial distance from the galactic center and r_o=8 kpc is the distance of the Sun. The scale height is H=325 pc, consistent with the counts of M dwarfs, and the scale length is h=3.5 kpc. The local stellar density ρ_o is given by

$$\rho_o = 0.336 \int_{M_{min}}^{M_{max}} \left(\frac{M}{0.1\ M_\odot}\right)^{-(1+x)}\ dM$$

where we have adopted a power law initial mass function $dN/dM \propto M^{-(1+x)}$ and the normalization factor at 0.1 $M_\odot$ is taken from Reid & Gizis (1997). The mass limits considered here are M_{min}=0.03 $M_\odot$ and M_{max}=0.8 $M_\odot$.

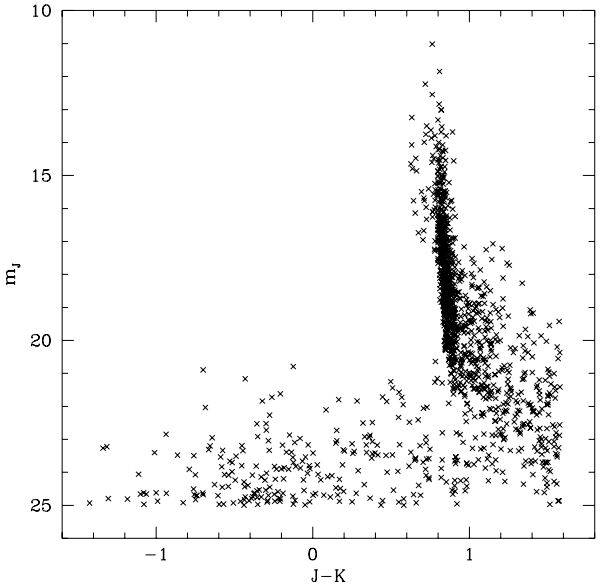

Fig. 6. Example of the predicted distribution of apparent stellar J magnitudes versus J–K colour for observations covering of 1 square degree. The points cluster along the main sequence defined by the thick part along J–K$\simeq$1, then we recognize the L–dwarfs which populate the region at 1<J–K<1.6, before evolving to much bluer colours when the methane bands begin to appear in the atmosphere.

In Eq. (1) the term $\Phi(T_{\rm eff}, {\rm M_J})$ gives the fraction of stars within the selected range of temperature and absolute J magnitude, i.e. the relative density of stars on a given position of the theoretical $T_{\rm eff}$–$\rm M_J$ HR diagram. This function, which depends on the shape of the IMF and on star formation history, is constructed via a Montecarlo technique assuming an uniform birth-rate from t=0 to the present disk age t_{disk}=10 Gyr. The program randomly extracts masses (with probability given by the chosen IMF shape) and ages from the track sets of Fig. 1. Each extraction provides a point in the $\rm M_{bol}$–$T_{\rm eff}$ diagram which translates into absolute magnitudes using the bolometric corrections of Table 1. The extracted stars are grouped into suitably small bins of temperatures and $\rm M_J$, this yields the matrix which represents the function Φ which is used to compute the integral of Eq. (1).

3.4. Results

The distribution of the apparent magnitude J as a function of the distance (Fig. 3) shows that the bulk of M dwarfs is at magnitudes J<20, where BDs begin to appear. L–dwarfs are numerous at J$\sim$20–22, while CH_4BDs begin to be common only at J>21.

Fig. 4 and Fig. 5 also show the same feature. The first displays the number counts per J magnitude within three mass bins: dwarfs (0.5–0.7 $M_\odot$), low mass dwarfs (0.08–0.14 $M_\odot$) and brown dwarfs (below 0.08 $M_\odot$). Being relatively bright, the dwarfs show a maximum in the distribution at J$\simeq$17, the lowest mass dwarfs also show a maximum at J$\simeq$20, while the BDs number increases down to the limit at which we count them (J=25). Therefore, either very deep searches are necessary to show an appreciable number of CH_4BDs, or a relatively deep survey covering most of the sky. Fig. 5 shows the total number counts versus J magnitude, putting into evidence which mass ranges contribute to its different parts. The broad maximum in the counts at J=17–19 includes only dwarfs and results from the combination of the effects due to the IMF, the mass luminosity relation for the main sequence and the radial density distribution. The rising of the number counts at J>22 is instead due to the low mass brown dwarfs. Finally, Fig. 6 shows simulated J vs J–K colour–magnitude diagram for observations covering 1 sq. degree of sky. The large scatter of J–K colours for the CH_4BDs reflects the effect of methane bands absorption on the J–K colour, which is expected to increase rapidly between $T_{\rm eff}$=1000 K (J–K=-0.1) and $T_{\rm eff}$=600 K (J–K=-1.4, see Table 1).

The resulting counts are tabulated in Table 2 for galactic coordinates similar to those of the ESO fields, namely b=55° l =340°, and at the galactic pole (b=90°).

3.5. Comparison with observations

Table 2 shows that a considerable number of L–dwarfs are predicted, but practically no CH_4BDs (at most 1 in 1000 sq. degrees), in a large area limited at K<14.5, in agreement with the early results of 2MASS. The very recent observations of four relatively bright CH_4BDs (Strauss et al. 1999, Burgasser et al. 1999) yields a surface density of $\simeq$0.002 cool methane dwarfs with J<16 and a factor of 3–6 lower than those predicted here using flat and steep IMFs, respectively, and considering only the density of objects of $T_{\rm eff}$<1400 K. However, these differences are not necessarily significant, given the small number of objects detected and the possibility that the the above searches may not be yet complete.

Our observed density of 3 objects with J<23.1 within 37 sq. arcmin is consistent (i.e. within the Poisson's noise) with the space density predicted using a relatively steep IMF ($x = 1$) while it is a factor of 4$\pm$2 larger than expected from a flatter IMF ($x = 0$). Remember that this latter IMF is certainly more consistent with the slope derived from nearby low mass stars (Reid & Gizis 1997). Given the very small number of objects detected we consider it premature to draw strong conclusions about the IMF.

4. Conclusions

We presented three CH_4BDs candidates with J<23.1 found in an area of 37 sq. arcmin covered by the ESO public images survey and modelled the expected number counts for these objects as well as for L and M dwarfs. Theoretical predictions are made on the basis of a sound galactic model including the most complete set of today's available evolutionary tracks and colours–$T_{\rm eff}$ correlations. The model could be significantly improved only when self–consistent computations will be available, including model atmospheres tested on the methane dwarfs which will be discovered.

Table 2. Predicted brown dwarf densities[(1)]

J_{lim}	CH_4BDs[a]	L [b]	M[c]	M[d]	M[e]	CH_4BDs[a]	L [b]	M[c]	M[d]	M[e]
IMF[f] x=0.0	l=0° b=90°					l=340° b=55°				
14.0	0.0004 + 0.0003	0.004	0.01	0.3	7	0.0004 + 0.0003	0.004	0.01	0.3	7
15.0	0.001 + 0.001	0.016	0.05	1	20	0.001 + 0.001	0.016	0.05	1	25
16.0	0.006 + 0.005	0.06	0.19	4	65	0.006 + 0.005	0.06	0.19	5	78
17.0	0.022 + 0.019	0.20	0.65	12	160	0.023 + 0.020	0.21	0.80	13	215
18.0	0.085 + 0.074	0.78	2.1	33	320	0.088 + 0.079	0.84	2.4	40	490
19.0	0.32 + 0.27	2.6	6.4	79	515	0.33 + 0.30	2.9	7.6	106	900
20.0	1.2 + 0.91	7.7	16	150	650	1.3 + 1.0	9.1	22	240	1300
21.0	4.0 + 2.7	19	34	230	702	4.4 + 3.2	25	51	420	1500
22.0	13 + 7.5	40	54	280	710	15 + 9.3	60	95	570	1550
23.0	38 + 16	74	73	290	710	50 + 20	115	130	570	1550
24.0	90 + 30	90	74	290	710	112 + 40	165	145	575	1550
25.0	160 + 38	90	74	290	710	270 + 72	200	150	575	1550
IMF[f] x=1.0	l=0° b=90°					l=340° b=55°				
14.0	0.0008 + 0.0006	0.006	0.018	0.3	3	0.0008 + 0.0006	0.006	0.018	0.3	3
15.0	0.003 + 0.002	0.025	0.068	1	9	0.003 + 0.002	0.025	0.070	1	9
16.0	0.01 + 0.009	0.1	0.25	4	32	0.01 + 0.009	0.1	0.25	4	32
17.0	0.045 + 0.036	0.31	0.9	12	68	0.046 + 0.036	0.32	0.9	13	90
18.0	0.17 + 0.13	1.2	3	32	140	0.18 + 0.14	1.3	3	40	210
19.0	0.69 + 0.48	4.0	8.5	75	240	0.72 + 0.54	4.5	10	105	400
20.0	2.3 + 1.6	12	22	150	310	2.5 + 1.8	14	28	230	600
21.0	8.0 + 4.9	30	44	225	345	9.0 + 5.7	39	66	400	720
22.0	25 + 13	61	69	270	350	29 + 17	94	120	550	760
23.0	84 + 24	99	73	270	350	95 + 47	170	150	550	760
24.0	200 + 38	125	76	270	350	240 + 95	235	170	560	760
25.0	385 + 52	130	76	270	350	535 + 130	270	170	560	760

[(1)] Cumulative number of objects per square degree with magnitude J$\leq$J$_{lim}$
[a] $T_{\rm eff}$<1400 K + 1400 K<$T_{\rm eff}$<1600 K
[b] 1600 K<$T_{\rm eff}$<2200 K
[c] 2200 K<$T_{\rm eff}$<2500 K
[d] 2500 K<$T_{\rm eff}$<3000 K
[e] 3000 K<$T_{\rm eff}$<3500 K
[f] IMF in the form $dN/dM \propto M^{-(1+x)}$

The predicted surface densities are in reasonably good agreement with the observed counts of L dwarfs and with the sparse observational data presently available for methane dwarfs, namely the lack of objects with K<14.5 in the early 2MASS survey, the recent finding of four relatively bright (J<16) CH_4BDs in 1800[2] sq. degrees and the three much fainter candidates discussed here.

We also showed that, due to their very low intrinsic luminosities, methane dwarfs become numerous (relative to L and M dwarfs) only at very faint J magnitudes (see figures from 3 to 6). To significantly improve the observational database it is therefore necessary to cover a reasonably large area of sky (several sq. degrees) down to J$\simeq$22, as well as K$\simeq$22 and I$\gtrsim$27, the latter two being necessary for selecting the CH_4BD candidates. We look forward for this type of observations to be soon performed by the IR large field deep imagers operating or planned on large telescopes.

Acknowledgements. We are grateful to ESO for making the EIS and NTT SUSI Deep field data available to the community. The EIS observations have been carried out using the ESO New Technology Telescope (NTT) at the La Silla observatory under Program-ID Nos. 59.A-9005(A) and 60.A-9005(A). This work was partly supported by the Italian Ministry for University and Research (MURST) under grant Cofin98-02-32. We thank A. Burrows for helpful discussion and G. Chabrier for a careful referee's report.

References

Allard F., 1998, In: Rebolo R., Martin E.L., Zapatero Osorio M.R. (eds.) Brown dwarfs and extrasolar planets. ASP Conference Series 134, 370

Arnouts S., D'Odorico S., Cristiani S., et al., 1999, A&A 341, 641

Bahcall J.N., Soneira R.M., 1978, ApJS 44, 73

Baraffe I., Chabrier G., Allard F., Hauschildt P.H., 1998, A&A 337, 403 (B98)

Burgasser A.J., Kirkpatrick J.D., Brown M.E., et al., 1999, ApJ 522, L65

Burrows A., Sharp C.M., 1999, ApJ 512, 843

Burrows A., Marley M., Hubbard W.B., et al., 1997, ApJ 491, 856

Burrows A., Sudarsky D., Sharp C., et al., 1998, In: Rebolo R., Martin E.L., Zapatero Osorio M.R. (eds.) Brown dwarfs and extrasolar planets. ASP Conference Series 134, 370
Chabrier G., Baraffe I., 1997, A&A 327, 1039 (CB97)
Cuby J.G., Saracco P., Moorwood A.F.M., 1999, et al., A&A 349, L41
da Costa L., Nonino M., Rengelink R., et al., 1999, submitted to A&A (astro-ph/9812105)
D'Antona F., Mazzitelli I., 1985, ApJ 296, 502
D'Antona F., Mazzitelli I., 1997, In: Micela G., Pallavicini R. (eds.) Cool stars in Clusters and Associations. Mem. Soc. Astron. Ital. 68, 807
Delfosse X., Tinney C.G., Forveille T., et al., 1999, A&AS 135, 41
Jones H.R. A., Tsuji T., 1998, In: Rebolo R., Martin E.L., Zapatero Osorio M.R. (eds.) Brown dwarfs and extrasolar planets. ASP Conference Series 134, 370
Kirkpatrick J.D., Beichmann C.A., Skrutskie M.F., 1998, ApJ 476, 311
Leggett S.K., Allard F., Hauschildt P.H., 1998, ApJ 509, 836
Leggett S.K., Toomey D.W., Geballe T.R., Brown R.H., 1999, ApJ 517, L139
Moorwood A.F.M., Cuby J.G., Lidman C., 1998, The Messenger 91, 9
Nakajima T., Oppenheimer B.R., Kulkarni S.R., et al., 1995, Nat 378, 463
Reid I.N., Gizis J.E., 1997, AJ 113, 2246
Reid I.N., Kirkpatrick J.D., Beichman C.A., et al., 1998, Proc. of the AAS meeting 192, #55.17
Rengelink R., Nonino M., da Costa L., et al., 1999, A&A 343, L29
Shaver P.A., Wall J.V., Kellermann K.I., Jackson C.A., Hawkins M.R.S., 1996, Nat 384, 439
Strauss M.A., Xiaohui F., Gunn J.E., et al., 1999, ApJ 522, L61
Tinney C.G., Delfosse X., Forveille T., Allard F., 1998, A&A 338, 1066
Tsuji T., Ohnaka K., Aoki W., Nakajima T., 1996, A&A 308, L29